Modes in a nonneutral plasma column of finite length

S. Neil Rasband and Ross L. Spencer

Citation: AIP Conference Proceedings **606**, 335 (2002); doi: 10.1063/1.1454302
View online: http://dx.doi.org/10.1063/1.1454302
View Table of Contents: http://scitation.aip.org/content/aip/proceeding/aipcp/606?ver=pdfcov
Published by the AIP Publishing

Modes in a Nonneutral Plasma Column of Finite Length

S. Neil Rasband and Ross L. Spencer

Department of Physics and Astronomy, Brigham Young University, Provo, Utah 84602

Abstract. A Galerkin, finite-element, nonuniform mesh computation of the mode equation for waves in a non-neutral plasma of finite length in a Cold-Fluid model gives an accurate calculation of the mode eigenfrequencies and eigenfunctions. We report on studies of the following: (1)finite-length Trivelpiece-Gould modes with flat-top and realistic density profiles, (2)finite-length diocotron modes with flat density profiles. We compare with the frequency equation of Fine and Driscoll [Phys Plasmas **5**, 601 (1998)].

INTRODUCTION

The familiar Cold-Fluid drift model for the nonneutral plasma gives inside the plasma the mode equation for the perturbed potential [1].

$$\frac{1}{r}\frac{\partial}{\partial r}(r\frac{\partial\Phi^{(1)}}{\partial r}) - \frac{m^2}{r^2}\Phi^{(1)} + \left(\left(1 - \frac{\omega_p^2(r)}{(\omega - m\omega_0)^2}\right)\frac{\partial^2\Phi^{(1)}}{\partial z^2}\right) + \frac{m\frac{\partial\omega_p^2(r)}{\partial r}}{\Omega r(\omega - m\omega_0)}\Phi^{(1)} = 0 \tag{1}$$

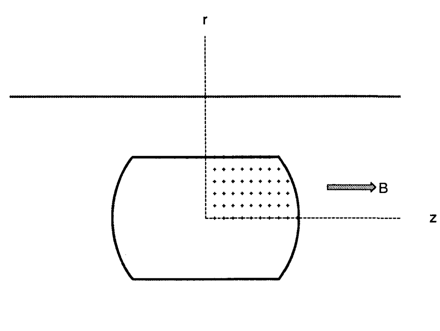

FIGURE 1. Region of Computation

CP606, *Non-Neutral Plasma Physics IV,* edited by F. Anderegg et al.

The computation region is illustrated in Figure 1 with $0 \leq r \leq r_{\text{wall}}$ and $0 \leq z \leq z_{\text{wall}}$, where the plasma in this region is confined to the region with the crosses.

Equation (1) can be written in the form

$$\nabla \cdot (\boldsymbol{\epsilon} \cdot \nabla \Phi^{(1)}) = 0,$$

where

$$\boldsymbol{\epsilon} = \begin{bmatrix} 1 & \frac{i}{\Omega} \int \frac{\frac{\partial \omega_p^2(r)}{\partial r}}{(\omega - m\omega_0(r))} dr & 0 \\ \frac{-i}{\Omega} \int \frac{\frac{\partial \omega_p^2(r)}{\partial r}}{(\omega - m\omega_0(r))} dr & 1 & 0 \\ 0 & 0 & 1 - \frac{\omega_p^2(r)}{(\omega - m\omega_0(r))^2} \end{bmatrix} \tag{2}$$

and

$$\Omega = \frac{qB}{mc}, \qquad \omega_0 = \frac{q}{m\Omega r} \frac{\partial \Phi_0}{\partial r}.$$

Construct a decomposition of the region of interest into triangular elements, *where the plasma boundary is approximated by edges of the triangles.* Figure 2 shows an example with $r_{\text{wall}} = 3.81\text{cm}$ and $z_{\text{wall}} = 30\text{cm}$.

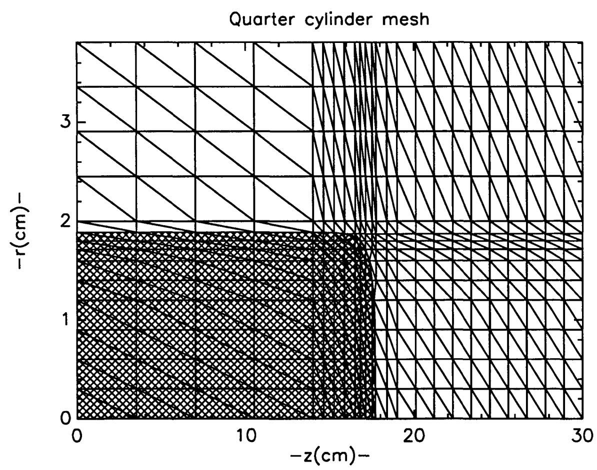

FIGURE 2. A triangulation of a plasma equilibrium. The region occupied by the plasma is shaded. Note that the scales for the vertical and horizontal axes are not the same.

Each triangle has 6 nodes (3 mid-points for the sides and 3 vertices) and on each node I a parabolic function:

$$\Psi_I(x, y) = \beta_1 + \beta_2 x + \beta_3 y + \beta_4 x^2 + \beta_5 xy + \beta_6 y^2.$$

This function is defined so that it has value 1 at the Ith node and 0 at all other nodes in the triangle. Then approximate $\Phi^{(1)}$ as a sum over nodes:

$$\Phi^{(1)}(x, y) = \sum_I C_I \Psi_I(x, y).$$

Boundary nodes have the C_I determined from boundary conditions on $\Phi^{(1)}(x,y)$.

The Galerkin integration of Eq.(1) multiplied by the approximating functions Ψ_J proceeds numerically by doing one triangular element at a time. If the element is outside the plasma, then $\boldsymbol{\epsilon} = \mathbf{1}$, otherwise it is as given in Eq.(2). This gives a matrix equation for the C_I.

$$\sum_I A_{JI} C_I = 0$$

with nonzero values of C_I only for certain values (eigenvalues) of ω. In practice we set

$$\sum_I A_{JI} C_I = 1, \qquad \text{for each} \quad J \tag{3}$$

and look for ω such that $\max(C_I) \to \infty$ or so that $1/\max(C_I) \to 0$.

TRIVELPIECE-GOULD (M=0) MODES

As a first example we present the results for a flat-top density profile with the plasma edge at $r_{\text{plasma}} = 1.89\text{cm}$, $z_{\text{plasma}} = 17.71\text{cm}$. The triangulation for this equilibrium is shown in Figure 2. The aspect ratio $\alpha = 9.37$ and $r_{\text{plasma}}/r_{\text{wall}} = 0.496$. For the modes that can be compared with the results in Table II of Jennings, Spencer, and Hansen [2] the agreement is excellent.

Figure 3 shows a scan in frequency for even modes in z with some of the prominent modes indicated.

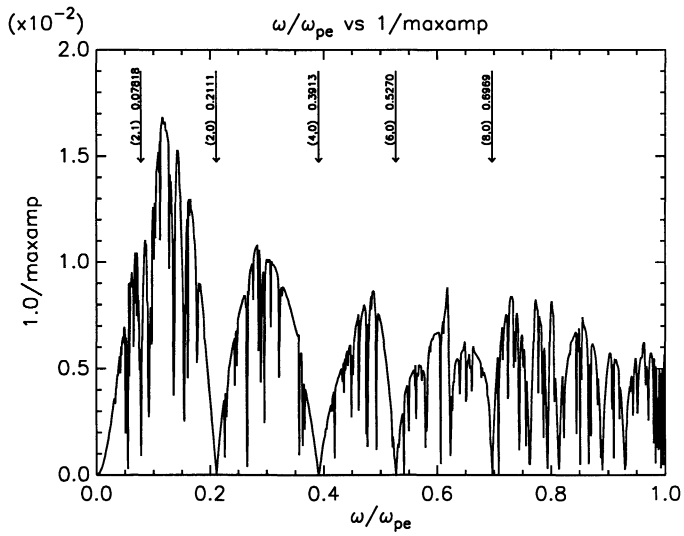

FIGURE 3. Scan of $1/\max(C_I)$ as described following Equation (3) for even modes.

A similar scan in frequency for the same equilibrium but odd modes gives frequencies $\omega/\omega_{pe} = 0.1079, 0.3060, 0.4630, 0.5766$ for the modes (1,0), (3,0), (5,0), and (7,0), respectively. Figure 4 shows the perturbed potential eigenfunctions for some of these modes.

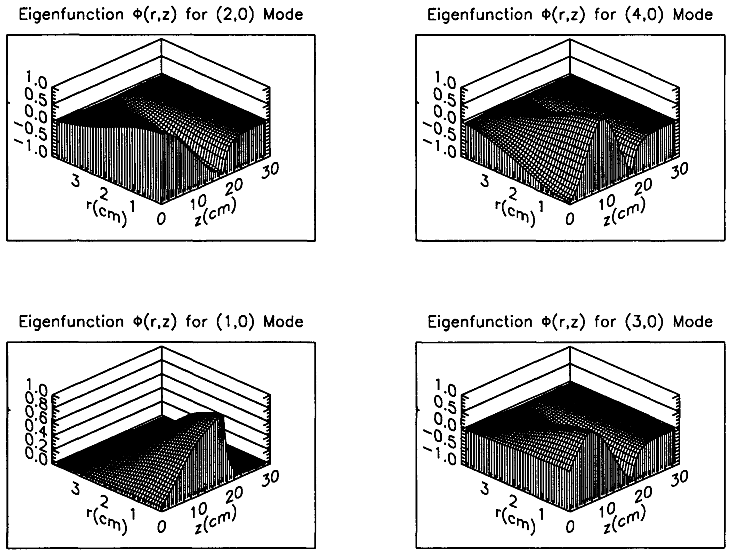

FIGURE 4. Perturbed potential eigenfunctions for selected modes

Lastly, for m=0 modes we consider briefly the effect of a radial dependence in the density profile. We compute equilibria [3] whose midplane density is

$$n(r)/n_0 = (1 - \sqrt{(1.5/\nu)(r/r_{\rm wall})^2}) \exp(-(r/r_l)^\nu).$$

We choose $r_l = r_{\rm wall}/2$ and compare two choices for ν, $\nu = 5.0, 40.0$, corresponding to a more-or-less average monotonic profile and a flat profile, respectively. Figure 5 shows the profiles with the corresponding (2,0) mode frequencies. The changes in the mode frequencies for such changes in density profiles are on the order of 10%.

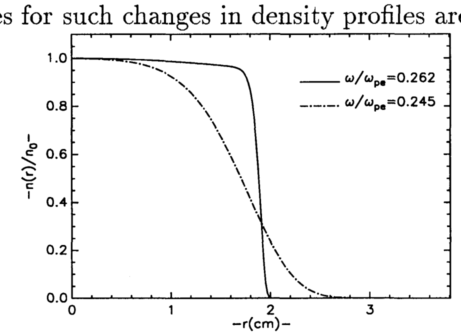

FIGURE 5. Density profiles and frequencies for (2,0) modes.

THE DIOCOTRON (M=1) MODE

We examined the finite-length diocotron mode frequency for a number of differing equilibria with varying plasma radii. All equilibria have flat-top density profiles and are computed in a Malmberg trap with radius $r_{\mathrm{wall}} = 3.81$cm, half-length $z_{\mathrm{wall}} = 30.0$cm and magnetic field 375 G. Figure 6 shows the shift in frequency from the infinite length result as a function of the plasma radius. This figure also compares these results to those obtained with the formula of Equation (24) in Fine and Driscoll [4].

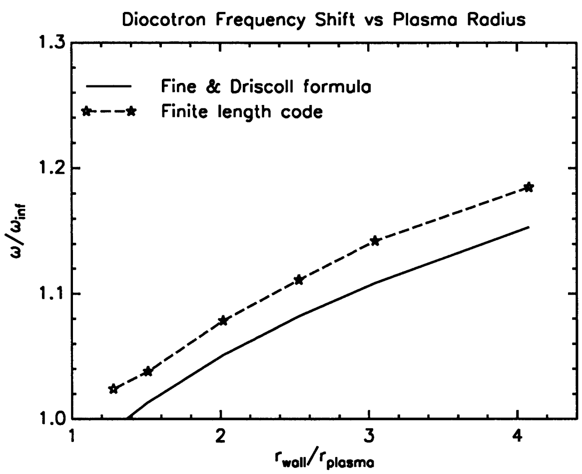

FIGURE 6. Diocotron frequency shift as a function of plasma radius.

For the case of $r_{\mathrm{wall}}/r_{\mathrm{plasma}} = 2.0$ Figure 7 shows the shape of the perturbed plasma potential in the quarter cylinder computation region. For a fixed z value less than the plasma half-length it is evident that inside the plasma the perturbed potential dependence on r is almost linear. A detailed examination of these eigenfunctions shows that inside the plasma their dependence on r is like $r + ar^3 + \cdots$ and in z like $1 + bz^2 + \cdots$ with a and b small for long plasmas. This is consistent with solutions inside the plasma that go like a modified Bessel function I_1 in r and $\cosh(kz)$ in z, with k very small corresponding to a wavelength much longer that the length of the confining cylinder [1].

This curvature in r is readily seen for a pancake-like equilibrium. In Figure 8 we show the edge curve for a pancake-like equilibrium with $r_{\mathrm{plasma}} = 2.524$cm and $z_{\mathrm{plasma}} = 0.138$cm for an aspect ratio of $\alpha = 0.055$. This Figure also includes a plot of the scaled perturbed potential as a function of r for a fixed value of z where the curvature is readily apparent. The m=1 diocotron mode for this equilibrium has a frequency of $\omega/\omega_{pe} = 0.00902$.

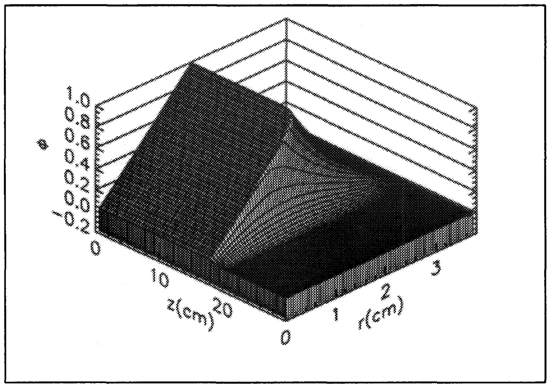

FIGURE 7. Perturbed Potential in the quarter cylinder for a m=1 diocotron mode

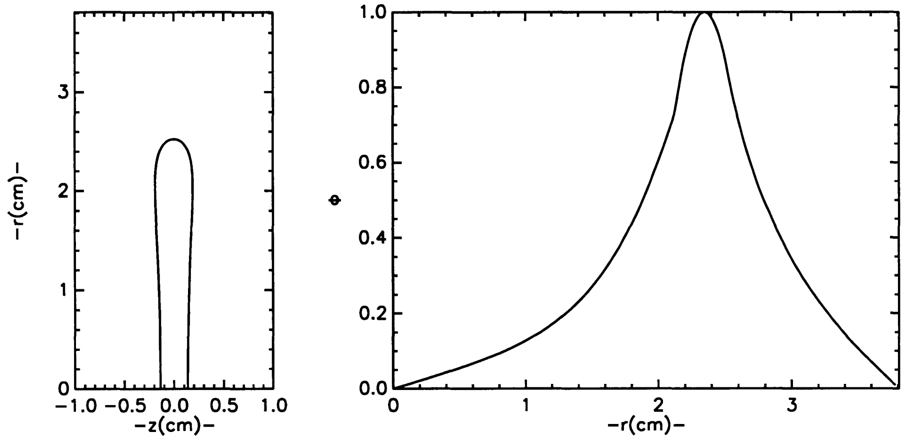

FIGURE 8. Pancake-like plasma edge and perturbed potential as a function of r for a fixed value of $z = 0.05$cm

REFERENCES

1. Prasad, S. A. and O'Neil, T. M.,*Phys. Fluids*, **26**, 665 (1983).
2. Jennings, J. K., Spencer, R. L., and Hansen, K. C., *Phys. Plasmas*, **2**, 2630 (1995).
3. Spencer, R. L., Rasband, S. N., and Vanfleet, R. R., *Phys. Fluids B*, **5**, 4267 (1993).
4. Fine, K. S. and Driscoll, C. F., *Phys. Plasmas*, **5**, 601 (1998).